Akademeia (2011) 1(1): ea0106

Physical Sciences
ARTICLE

Piezoelectric field effects on sensitivity of Hall sensors based on AlGaAs/InGaAs/GaAs heterostructures

Lofti Bouzaïene[‡a], Larbi Sfaxi [a], and Hassen Maaref [a]

[a] *Laboratoire de Micro-optoélectronique et Nanostructures, Faculté des Sciences de Monastir, Université de Monastir, Monastir 5000, Tunisia*

The sensitivity and performance of Hall sensors depends on the electron mobility of its substrate. With the aim to design a substrate capable of operating at high-absolute magnetic sensitivity and high current-related sensitivity we investigated the theoretical consequences of utilizing a high-index GaAs substrate in AlGaAs/InGaAs/GaAs heterostructures. The shape of the confining potential, the sub-band energies, the eigen envelope wave functions, and the Fermi energy in the InGaAs channel were calculated self-consistently at low temperature, taking into account exchange-correlation, strain, and piezoelectric effects. The piezoelectric field significantly increased the electron density (n_s) in the channel when the structure was grown on a GaAs (111)A substrate. This implies that one can have a wider spacer layer without altering n_s, with the result of enhanced electron mobility. These data suggest that AlGaAs/InGaAs/GaAs heterostructures have high electron mobility and low sheet electron density, and are suitable for a highly-sensitive Hall sensor.

KEYWORDS: Piezoelectric field; Hall sensors; sensitivity; AlGaAs/InGaAs/GaAs heterostructures

During the last decade, several studies have been carried out using highly sensitive Hall sensors [1,2]. The new generation of Hall sensors has played a special role in elucidating quantum well structures with two dimensional electron gas (2DEG) in the conduction channel. The high electron mobility of the 2DEG is advantageous primarily within low electric fields [3]. A highly sensitive Hall device with a large signal-to-noise (S/N) ratio and a small temperature coefficient can be obtained by combining high electron mobility with moderate sheet carrier density [4,5]. AlGaAs/InGaAs/GaAs heterostructures deserve special attention in this respect. Structures grown on substrates with orientations different from (001) possess built-in piezoelectrically generated electric fields. When III-V heterostructures are grown on (N11) substrates it provides a further degree of freedom for electro-optical devices [6]. In doped AlGaAs/InGaAs/GaAs heterostructures, optimal Hall sensor performance depends on high electron mobility. This can be attained by using a high-index substrate. In our previous works [7,8] we demonstrated enhanced mobility and electron density of structures grown on (111)A GaAs substrate compared to equivalent (001) substrates. The aim of the present report was to modify the high-index substrate (111)A in a way that will increase electron mobility without decreasing carrier density. We report on the design of a 2DEG Hall sensor based on an AlGaAs/InGaAs/GaAs heterostructure for two different growth directions, namely (001) and (111)A. This Hall sensor is optimized particularly with respect to measurement of low magnetic fields.

[‡] Correspondence: lotfi.bouzaiene@fsm.rnu.tn
Received: 15 October 2010; **Accepted:** 01 April 2011

Device structure

A semiconductor structure was made of a Si δ-doped AlGaAs barrier layer, an InGaAs thin layer (channel), and a p-type GaAs buffer layer grown on two different GaAs substrate orientations, (001) and (111)A. The Si δ-doped layer with a Si sheet concentration of 2×10^{12} cm^{-2} was separated from AlGaAs/InGaAs heterointerface by a variable spacer layer thickness (**fig. 1**). The role of the undoped spacer layer was to increase the electron mobility by separating the ionized donor atoms from the confined electrons in the InGaAs channel. The conduction electrons are located in the two dimensional channel formed by InGaAs layer with a thickness of (10 – 15 nm). The value of the channel width is dictated by the optimal In composition (0.1 to 0.3) from the point of view of quality of the crystal structure. Larger thickness in strained structures with the same In compositions were avoided as they can give rise to lattice defects.

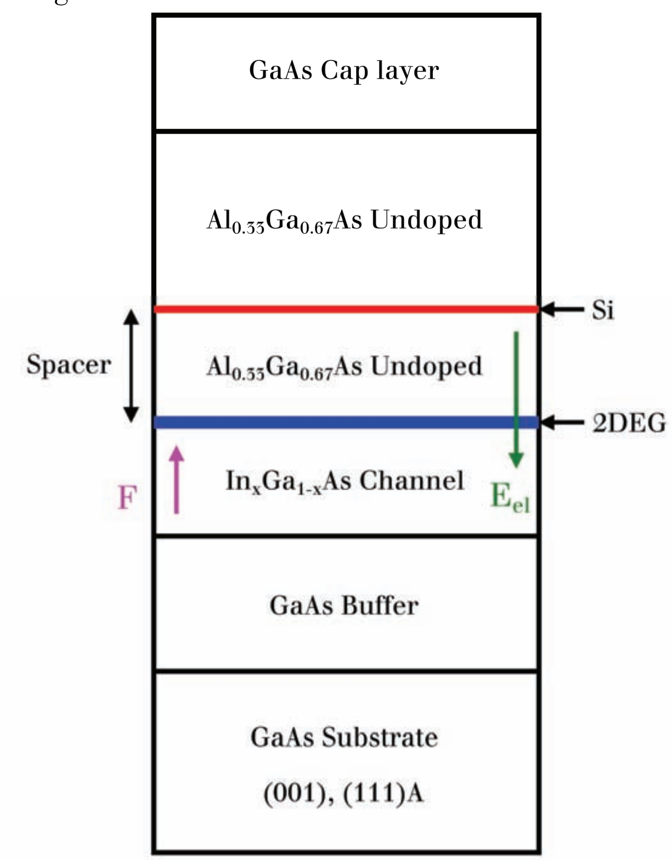

Figure 1. Schematic cross section of the Si δ-doped $Al_{0.33}Ga0.67As$/InGaAs/GaAs structure based Hall sensor on two different GaAs substrate, (001) and (111)A.

Theoretical formulations

Theoretical calculations were concerned with the self-consistent study of Si δ-doped AlGaAs/InGaAs/GaAs heterostructures, for two different GaAs substrate orientations, (001) and (111)A, used here as Hall sensors. We assumed the validity of the effective mass approximation and take an isotropic and parabolic conduction band in the growth direction. The problem was solved by reducing a series of one-dimensional equations. Quantized energy levels and the 2DEG concentration were given by simultaneously solving the Schrödinger-Poisson equations:

$$-\frac{\hbar^2}{2}\frac{d}{dz}\left(\frac{1}{m^*(z)}\frac{d}{dz}\right)\psi_i(z)+U(z)\psi_i(z)=E_i\psi_i(z)$$
$$\frac{d}{dz}\left(\varepsilon(z)\frac{d}{dz}U_H(z)\right)=\frac{e^2}{\varepsilon_0}\left[N_D(z)-N_A(z)-n(z)\right] \quad (1)$$

The potential U(z) is divided into four different contributions:

$$U(z) = U_b(z) + U_H(z) + U_{XC}(z) + U_{pz}(z) \quad (2)$$

where $U_b(z)$ represents the conduction band discontinuity without doping, $U_H(z)$ is the Hartree potential obtained by solving the Poisson equation, $U_{XC}(z)$ is the exchange-correlation potential, and $U_{pz}(z)$ is the piezoelectric potential [8].

Here z is the growth direction, $m^*(z)$ is the electron effective mass at the bottom of the Γ valley, and ε(z) is the local dielectric constant of the different layers. E_i and ψ_i are the quantized energy levels and corresponding electronic wave functions respectively. $N_D(z)$ in the total density of ionized dopants, $N_A(z)$ is the residual acceptor concentration in the unintentionally doped GaAs, and n(z) is the local density of the confined electrons,

$$n(z)=\sum_i n_i\left|\psi_i(z)\right|^2 \quad (3)$$

At low temperature, n_i can be written as

$$n_i=\frac{m^*}{\pi\hbar^2}\left(E_F-E_i\right) \quad (4)$$

where n_i is the carrier population in the i^{th} subband and E_F is the Fermi level. At low temperature, E_F is pinned at the DX center energy [9].

Therefore, the total sheet electron density in the channel, n_s, is the sum of the carrier population in all subbands, and can be written as follows:

$$n_s=\sum_i n_i \quad (5)$$

The exchange-correlation potential which is induced by the many-body effects and whose expression is taken from [10]:

$$U_{xc}(z) = -0.916\frac{e^2}{6\pi\varepsilon_0\varepsilon_r}\left[\frac{3n(z)}{4\pi}\right]^{\frac{1}{3}} \quad (6)$$

where $U_{pz}(z)$ is the piezoelectric potential that can be written as:

$$U_{pz}(z) = eFz \quad (7)$$

Here F is the magnitude of the piezoelectric field in the strained InGaAs layer. The piezoelectric field for a (111)A oriented substrate is proportional to the lattice mismatch between the GaAs and InGaAs layers and is represented by the equation [11]:

$$F = \frac{2\sqrt{3}e_{14}\left(c_{11} + 2c_{12}\right)}{\varepsilon_0\varepsilon_r\left(c_{11} + 2c_{12} + 4c_{44}\right)}\delta \quad (8)$$

with the lattice mismatch $\delta = \frac{a_{GaAs} - a_{InGaAs}}{a_{InGaAs}}$, where c_{11}, c_{12}, and c_{44} are the elastic stiffness tensor coefficients and e_{14} is the piezoelectric coefficient (see [12]).

In evaluating the total potential, we have taken into account the strain effects by using the following equations [13]:

$$\begin{aligned} \Delta E_c &= A_c\left(e_{11} + e_{22} + e_{33}\right) \\ A_c &= -8.8 + 1.05x + 0.45x^2 \end{aligned} \quad (9)$$

where A_c is the conduction deformation potential, x is the In concentration in the channel (InGaAs), and e_{ii} are the strain-tensor elements.

For the high-symmetric (001), and (111) growth directions, the strain-tensor elements are as follows [14]:

$$(001):\ e_{11} = e_{22} = \delta,\ \ e_{33} = -\frac{2c_{12}}{c_{11}}\delta; \quad (10)$$

$$(111):\ e_{11} = e_{22} = e_{33} = \frac{4c_{44}}{c_{11} + 2c_{12} + 4c_{44}}\delta; \quad (11)$$

The same theoretical method (finite differential method) was adopted in our previous analyses [15].

Results and Discussion

If a Hall sensor with a 2DEG active layer is supplied with constant bias current, and for Greek-cross shape structures [16], the Hall voltage U_H [17] and the current-related sensitivity S_I read:

$$U_H = S_I BI, \quad S_I = \frac{1}{en_s} \quad (12)$$

where I is bias current, B is the perpendicular part of the incident magnetic field, n_s is the sheet electron density, and the e the electronic charge. Thus,

$$U_H \approx \mu.E.W.B \quad (13)$$

where μ is the electron mobility, E the electric field in the active region of the Hall device, and W the width of the active region.

The latter relationship shows that the absolute sensitivity of the Hall sensor,

$$S_A = \frac{dU_H}{dB} \approx \mu.E.W \quad (14)$$

Therefore semiconductors which have high electron mobilities and small sheet electron densities are desirable for a highly-sensitive (S_A and S_I) Hall sensor. Heterojunction semiconductors with 2DEG ideally satisfy these conditions [18]. However, a low n_s has a detrimental effect in increasing sensor noise [19].

As a system, we consider a Si δ-doped $Al_{0.33}Ga_{0.67}As/In_xGa_{1-x}As/GaAs$ structure based Hall sensor for two different GaAs substrate orientations, such as (001) and (111)A. We have calculated for these heterostructures the conduction band edge, the energy spectrum and wave functions of the confined electronic states. The subbands have been computed self-consistently, at low temperature, with variable In composition, spacer thickness and InGaAs channel width parameters. In all cases the the donor concentration is fixed at $2x10^{12}$ cm^{-2}.

Figure 2 shows the shape of the conduction-band, the subband energies, the eigen envelope wave functions and the Fermi level, calculated at low temperature, of a Si δ-doped AlGaAs/InGaAs/GaAs heterostructure grown on (001) GaAs substrate. The spatial separation between the δ-doped layers and the AlGaAs/InGaAs heterointerfaces (spacer) is fixed at 10 nm.

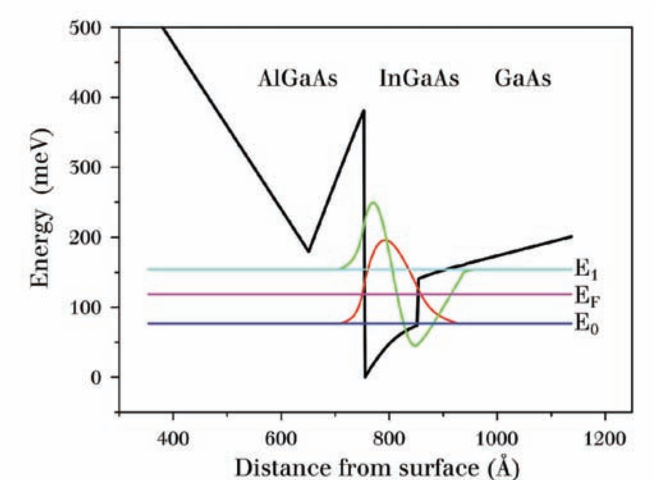

Figure 2. The self-consistent calculation of the conduction band structure, the levels energy, the corresponding envelope wave functions, and the Fermi level for Si δ-doped $Al_{0.33}Ga_{0.67}As/In_{0.15}Ga_{0.85}As/GaAs$ Hall sensor structure grown on (001) GaAs oriented substrate. With donor concentration $N_D^{2D} = 2x10^{12}$ cm^{-2}, channel thickness = 10 nm, and spacer = 10 nm at low temperature.

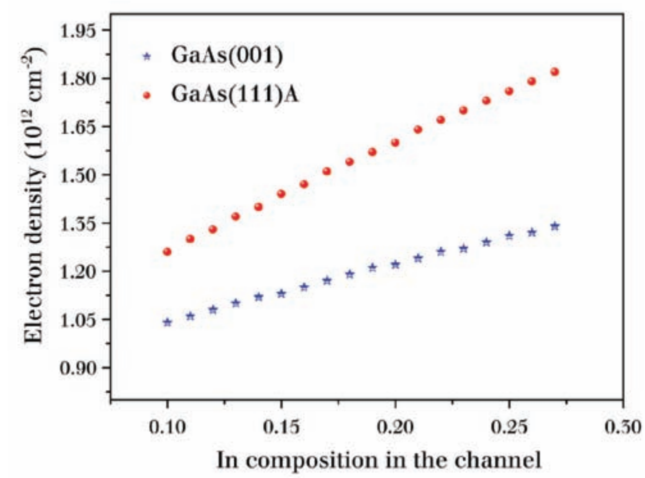

Figure 3. Variation of the electron density, at low temperature, as a function of the In composition in the channel with L_{InGaAs} = 10 nm, and spacer layer = 10 nm.

The electrons in the InGaAs channel are separated from the donors in the AlGaAs barrier by a thin spacer layer, which decreases the impurity scattering, and enhances the electron mobility [20,21]. Indeed, a higher value of the electron mobility can be obtained by increasing the spacer layer thickness. In fact, the latter controls the amount of electron concentration trapped in the channel, n_s, and hence the current-related sensitivity (S_I). However, the cost of such enhancement is a drastic decrease of electron density in the InGaAs channel, leading to a very high resistive device.

In our previous works [7,22], we showed electron density in a pseudomorphic high electron mobility transistor (pHEMT) may be enhanced by utilising (111)A GaAs substrate instead of (001) GaAs. The 2DEG concentration calculated by solving the Schrödinger-Poisson equations self-consistently is plotted in **figure 3** as a function of the In composition in the InGaAs channel, with a fixed well thickness of 10 nm, for the (001) and (111)A GaAs substrates. This demonstrates immediately that the calculated electron density in the structure grown on a (111)A GaAs substrate is significantly higher than that grown on (001) GaAs substrate. Moreover, this enhancement holds for several different indium concentrations.

As a result we noted a significant 30% increase in the electron density between (111)A and (001) growth directions when the In composition was equal to 0.25. This improvement was due to the incorporation of a piezoelectric field, oriented toward the surface, within the strained active layer (InGaAs) in the structures grown on (111)A GaAs substrates.

Spacer layer thickness, InGaAs channel width, and GaAs substrate orientation were varied for each structure. The following four sets of conditions were considered:

(a) spacer layer thickness was selected to be 10 nm, and InGaAs channel width was fixed at 10 nm. GaAs substrate orientation, (001).
(b) spacer layer thickness was selected to be 10 nm, and InGaAs channel width was fixed at 10 nm. GaAs substrate orientation, (111)A.
(c) spacer layer thickness was selected to be 16 nm, and InGaAs channel width was fixed at 10 nm. GaAs substrate orientation, (111)A.
(d) spacer layer thickness was selected to be 23 nm, and InGaAs channel width was fixed at 15 nm. GaAs substrate orientation, (111)A

The calculated results are reported in **figure 4**, corresponding to the above four conditions. Each figure displays the self-consistent conduction band edge, the leading two energy levels as well as the corresponding wave functions, and the Fermi level.

In **table I**, we show the calculated 2DEG concentration in the InGaAs channel for the same samples (a)-(d). Sample (a) represents a conventional AlGaAs/InGaAs/GaAs based magnetic Hall sensor, grown on GaAs (001) substrate, used here as reference. Sample (b), which has the same spacer thickness but is grown on GaAs (111)A substrate, exhibits higher electron density.

Table 1. Electron density in the channel of the Hall sensor structure for different spacer thickness. Sample a represents the conventional structure grown on (001) GaAs substrate. Sample d exhibits the same n_s as sample a, but has larger spacer thickness, leading to much higher device sensitivity grown on (111)A GaAs substrate.

Sample	GaAs substrate orientation	Spacer thickness/ channel width	x_{In}	n_s (10^{12} cm^{-2})
(a)	(001)	10 nm / 10 nm	0.15	1.09
(b)	(111)A	10 nm / 10 nm	0.15	1.44
(c)	(111)A	16 nm/ 10 nm	0.15	1.08
(d)	(111)A	23 nm/ 15 nm	0.15	1.07

For the (001) growth direction there was no piezoelectric field. The potential was deeper to the left near the doped AlGaAs barrier and the first wave function ψ_0 was displaced towards the left. In the (111)A growth direction however there was a piezoelectric field oriented toward the surface (N.B. F and the depletion field E_{el} was in opposite directions), giving a potential much deeper to the right, near the GaAs undoped barrier. In this growth scenario electrons are concentrated to the right half of the InGaAs channel layer.

The spatial charge distribution in the InGaAs channel was strongly influenced by the presence of the built-in piezoelectric field. We observed the displacement of the envelope wave function $\psi_0^{(111)A}(z)$ maximum to the right by 7.6 nm when the $In_{0.15}Ga_{0.85}As$ well thickness was equal to 15 nm in relation to $\psi_0^{(001)}(z)$. This displacement was predicted to improve the spatial separation between confined electrons in the channel and the ionized dopants in the AlGaAs barrier (an increase of the spacer: L_s). After the spacer was increased, the electron mobility increased too, as the latter is approximately proportional to $L_s^{5/2}$ [23] or L_s^3 [20,21]. The relationship between the electron mobility and the undoped spacer layer is

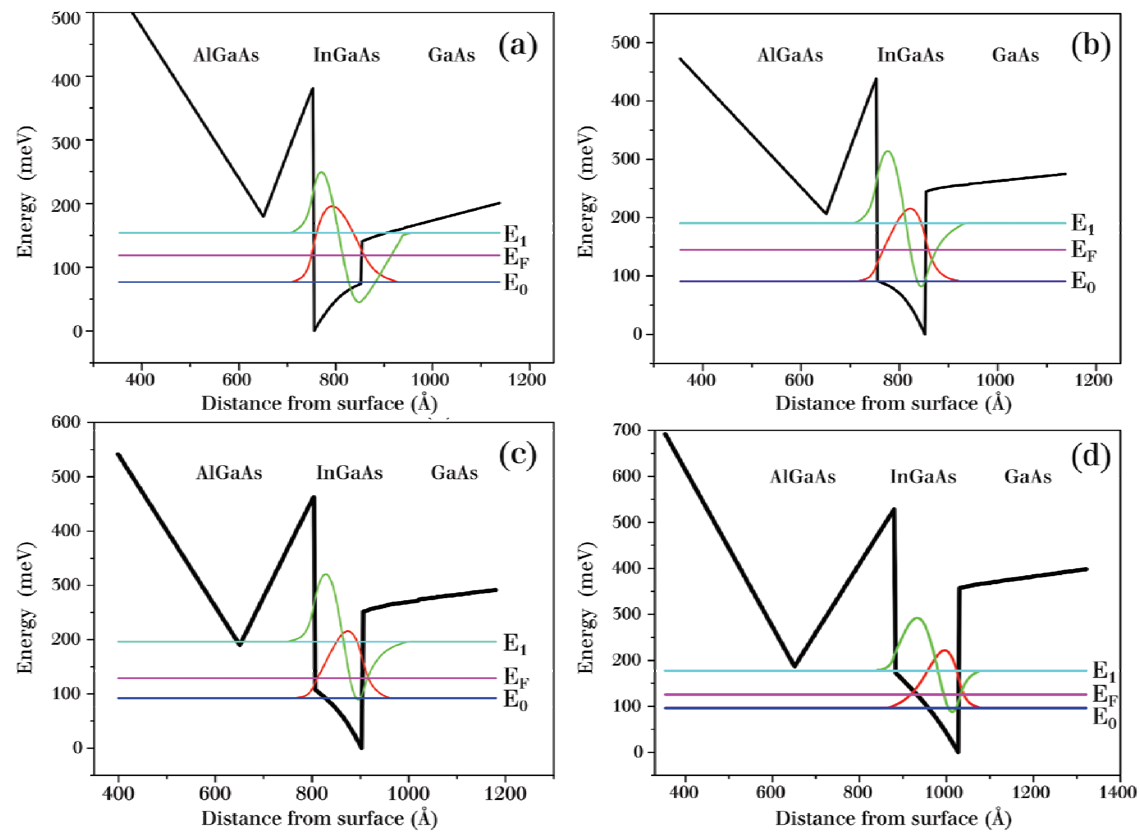

Figure 4. The self-consistent calculation, at low temperature, of the conduction band structure, levels energy, corresponding envelope wave functions, and Fermi level for δ-doped $Al_{0.33}Ga_{0.67}As/In_{0.15}Ga_{0.85}As/GaAs$ Hall sensor structure, with donor concentration $N_D^{2D} = 2x10^{12}$ cm^{-2}.

(a) With channel thickness = 10 nm, spacer = 10 nm and grown on (001) GaAs oriented substrate.
(b) With channel thickness = 10 nm, spacer = 10 nm and grown on (111)A GaAs oriented substrate.
(c) With channel thickness = 10 nm, spacer = 16 nm and grown on (111)A GaAs oriented substrate.
(d) With channel thickness = 15 nm, spacer = 23 nm and grown on (111)A GaAs oriented substrate. Sample d is the proposed Hall sensor structure.

$\mu \propto \frac{k_F^3 d_i^3}{N_i}$. N_i is the ionized charge centres per surface unity situated at distance d_i from an electron gas of Fermi wave vector k_F. The electron density n_s is accordingly related to the Fermi wave vector k_F by $n_s = \frac{k_F^2}{2\pi}$ for a two dimensional system at 0K. This relation is also valid for uniformly doped and δ-doped structures at low temperature.

Thus sample (b) features better absolute sensitivity (SA) of the Hall sensor than sample (a), since SA is proportional to μ. However, we noted an enhancement of the electron density, leading to a drastic decrease of the current-related sensitivity, SI. Sample (c), which has the same InGaAs channel width (10 nm) but the spacer layer thickness was selected to be 16 nm grown on GaAs (111)A substrate, exhibits the same electron density with sample (a). Therefore, the spacer increases. Sample (d) represents the proposed structure. Compared to the conventional structure, the innovative structure shows wider spacer thickness (30 nm, is the sum of spatial separation between the ionized dopants in the AlGaAs barrier at AlGaAs/InGaAs interface and the displacement of the envelope wave function ψ0(111)A(z) maximum relation to ψ0(001)(z)), the same electron density in the InGaAs channel and grown on GaAs (111)A substrate. Therefore, SA is enhanced and SI remains unchanged, since ns is the same for both samples (a) and (d). The results reported in Table I show that absolute magnetic sensitivity may be increased by

$$\frac{\mu_d}{\mu_a} \approx \left(\frac{spacer_d}{spacer_a}\right)^{\frac{5}{2}} = \left(\frac{L_s^d}{L_s^a}\right)^{\frac{5}{2}} \approx 8$$

where μ_d and μ_a are, respectively, the mobility of samples (d) and (a) and L_s^d and L_s^a are, respectively, the spacer layer thickness of sample (d) and (a). Thus the proposed structure (d) can be used to fabricate highly sensitive Hall sensor.

Conclusion

We present a novel structure for a Hall sensor with enhanced sensitivity. In the proposed design the electron mobility was increased without decreasing the 2DEG concentration by means of using a (111)A GaAs instead of (001) GaAs substrate, and by widening spacer layer thickness. Charge density profiles, total two dimensional electron densities, and sensitivities of this proposed substrate arrangement were calculated by solving the Schrödinger and Poisson equations self-consistently. We calculate that with the proposed changes in sensor substrate design, absolute magnetic sensitivity can be enhanced by a factor of 8 over a reference sensor design. Furthermore, this design allows for the current-related sensitivity to be optimized for suitable chosen spacer thickness. These results suggest that highly sensitive Hall sensors can be designed based on AlGaAs/InGaAs/GaAs heterostructures grown on (111)A GaAs substrates.

References

1. Boero *et al.*, Sens. Actuators A 106 (2003) 314.
2. A. Geim *et al.*, Nature 396 (1998) 144.
3. Y. Sugiyama, H. Soga, and M. Tanaco, J. cryst. Growth 95 (1989) 394.
4. V. Mosser, S. Contreras, S. Abdoulhouda, Sens. Actuators A 43 (1994) 135.
5. J. S. Lee, K. H. Ahn, Y. H. Jeong, D. M. Kim, Sens. Actuators A 57 (1996) 183.
6. P. O. Vaccaro, M. Takahashi, K. Fujita, T. Watanabe, Jpn. J. Appl. Phys. 34, Part 2 (1995) L13.
7. L. Bouzaïene *et al.*, Appl. Phys. A 80 (2005) 295.
8. L. Bouzaïene *et al.*, Eur. Phys. J. Appl. Phys. 29 (2005) 209.
9. A. Leuther, A. Föster, H. Lüth, H. Holzbercher, U. Breur, Semicond. Sci. Technol. 11 (1996) 766.
10. P. Ruden, G. H. Dohler, Phys. Rev. B 27 (1983) 3538.
11. T. S. Moise, L. J. Guido, J. C. Beggy, T. J. Cunningham, J. Electron. Mater. 21 (1992) 119.
12. P. O. Vaccaro, K. Tominaga, M. Hosoda, Jpn. J. Appl. Phys. 34 (1995) 1362, Part 1, 2B.
13. C. Kopf, H. Kosina, S. Selberherr, Solid State Electron. 41 (1997) 1139.
14. E. A. Caridi, J. B. Stark, Appl. Phys. Lett. 60 (1992) 1441.
15. L. Bouzaëne, L. Sfaxi, H. Sghaeir, H. Maaref, J. Appl. Phys. 85 (1999) 8223.
16. R. S. Popovic, Hall Effect Devices, Adam Hilger, Bristol, (1991), pp. 165-170.
17. R. Boll, K. J. Overshott, Magnetic Sensors, Verlagsgesellschaft mbH, D-6940 Weinheim, (1989).
18. Y. Sugiyama, T. Taguchi, M. Tacano. In : Proc.6th Sensor Symp. (1986) 55.
19. V. P. Kunets et al, Sens. Actuators A 101 (2002) 62.
20. T. Ando, B. Fowler, and F. Stern, Rev. Mod. Phys. 54 (1982) 437.
21. B. Etienne, E. Paris, J. Phys. 48 (1987) 2049.
22. S. Rekaya, L. Bouzaïene, L. Sfaxi, H. Maaref, Appl. Phys. A 81 (2005) 79.
23. K. Lee and M. S. Shur, J. Appl. Phys. 54 (1983) 6432.